JOURNAL OF SOLID STATE CHEMISTRY 51, 388–395 (1984)

Temperature Dependence of the Solubility Limit of Chromia (Cr_2O_3) in Titania (TiO_2)

L. A. BURSILL AND SHEN GUANG JUN

School of Physics, University of Melbourne, Parkville, 3052, Victoria, Australia

Received July 28, 1983; in revised form October 4, 1983

Electron microscopic observations are made to establish (i) that $(Ti,Cr)O_{2-x}$ is a true nonstoichiometric phase, containing small defects, coherent with and highly mobile within the rutile lattice, such small defects being effectively randomized homogeneously throughout the lattice, and (ii) the approximate temperatures for small/extended defect equilibria in $(Ti,Cr)O_{2-x}$ ($0 \leqq x \leqq 0.05$), using a novel technique for the determination of the temperature and stoichiometry dependence of the phase limits. These results are readily interpreted in terms of linear cationic interstitial small defect models.

I. Introduction

Phase analysis studies of chromia (Cr_2O_3) in titania (TiO_2) show a remarkable degree of solid solubility (up to 7.5 mol.% $CrO_{1.5}$ at 1770 K) (*1–5*). Thus a net anion deficiency appears to be accommodated as randomized point defects or defect complexes. Electron microscopic studies (*3, 4*) suggested that specimens initially showing no extended defects (after quenching from 1773 K) may precipitate lamellae of CSP (crystallographic shear planes) on annealing at lower temperatures. Philp and Bursill (*4*) concluded that the critical concentration for which CSP start to precipitate should decrease with decreasing temperature. O'Keeffe and Ribble (*2*) studied the solubility limit of chromia in rutile for 1273–1773 K using interdiffusion couples and electron microprobe measurements. Somiya *et al.* (*5*) reported ~7.5 wt% Cr_2O_3 solubility limit throughout the temperature range 1673–1923 K. They also showed that Cr_2O_3 is lost on annealing sintered pellets in air.

In this paper a novel technique is described for the determination of the extent of the $(Ti,Cr)O_{2-x}$ phase as a function of temperature. This offers a sensitive method of detection of CSP precipitation, using lattice imaging and electron diffraction data, and at the same time allows the stoichiometry of the precipitated phase to be measured, thus overcoming problems associated with loss of Cr_2O_3 with respect to the bulk analyses. The temperature range 523–1773 K was investigated. A new model for the nature of the "small defect" structures responsible for the nonstoichiometric phase $(Ti,Cr)O_{2-x}$ is discussed.

II. Experimental Method

The starting materials were Cr_2O_3 powder (Koch-Light,3N) and slices of a single

0022-4596/84 $3.00

crystal rutile (TiO_2) boule (National Lead Co.). These were weighed and the slices were loaded for powder to give initial overall stoichiometries $MX_{1.995-1.94}$ (for details see Table I). The loaded slices were then wrapped carefully in platinum foil and heated at 1773 K for 1 or 2 days (specific details given in Table I). In each case the chromia appeared to have reacted completely with the rutile, since there was no unreacted powder in the platinum containers. However, following the results of Ref. (*5*), we expect that some chromia may have been lost by sublimation, evaporation, or distillation (see Table I). The products appeared mostly homogeneous in color, although thin sections of the less-doped specimen $MX_{1.995}$ showed gradations in color. Smaller pieces ($\cong 2 \times 1 \times 1$ mm) of each slice were then given a variety of heat treatments in sealed platinum tubes. At the end of each treatment the specimens were removed rapidly from the furnace, by pulling quickly on a platinum wire, and cooled in contact with a metal block. The temperature fell to $\leqq$ 350 K in $\leqq \frac{1}{2}$ min. *In situ* heating experiments in an electron microscope had established previously that such specimens were not reactive for temperatures $\leqq$ 670 K (*6*).

Specimens were prepared for electron microscopy by crushing fragments in an agate mortar with pestle, under chloroform, and allowing a drop of the resulting dispersion to dry onto a holey-carbon support film. Thin areas were selected and oriented into ⟨100⟩, ⟨111⟩, ⟨101⟩, or ⟨001⟩ zone axis projections. A JEOL-100CX electron microscope, fitted with a high-tilt side-entry goniometer (±60°, ±45° tilts), was employed.

III. Results

Specimens reacted at 1773 K showed *no* CSP or other precipitate-type contrasts. ({011} Twin-lamellae sometimes occurred, but these were associated with mechanical twinning, induced by high local stresses during crushing—see Ref. (*7*) for some high-resolution observations and characterization of these defects.) Samples of each of the initial reactions were then annealed at successively lower temperatures and observed electron optically until precipitation of CSP occurred. The time evolution of precipitation is illustrated in Fig. 1, for $(Ti,Cr)O_{1.98}$ annealed at 873 K. Thus, no extended defects were visible in specimens cooled rapidly from 1773 K (Fig. 1a); {253} CSP precipitated[1] after 15 min at 873 K (Fig. 1b) giving rise to short ($\cong$200–400 Å) line contrast features. Some coarsening of this texture occurred after 3 hr at 873 K but further changes did not become apparent after annealing at 873 K for 22 hr (Fig. 1c); although some areas, including that illustrated here, showed extensive wedge fringes, possibly indicating development of CSP lamellae (cf. Fig. 2a below).

On annealing for 1–2 days at temperatures just below the phase limit (e.g., 1073 K for $MX_{1.98}$) extensive CSP lamellae appeared (Fig. 2a). The corresponding [111] zone axis diffraction pattern showed rows of sharp superlattice spots along $\mathbf{k}_{253}$ (Fig. 2b). Measurements of CSP spacings yielded D_{SP} = 55 Å and stoichiometry $(Ti,Cr)O_{1.977}$, in good agreement with the nominal stoichiometry in this case.

Further heating experiments (Table I) then established the precipitation temperatures for different stoichiometries. Specimens were heated for 17–24 hr in order to induce relatively well-ordered CSP structures. Figures 3a–f illustrate changes in the [111] zone axis patterns as a function of stoichiometry and temperature. Annealing for periods of $\geqq$ 1 day produced some coarsening of the lamellae textures, but no significant changes in CSP ordering.

[1] CSP orientations were determined using ⟨111⟩ zone axis diffraction patterns, see Refs. (*4*, *8*).

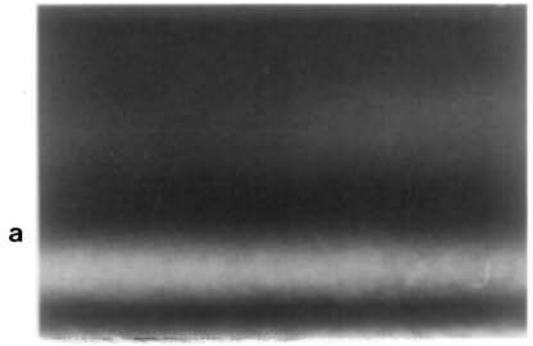

Specimens containing CSP (in $y > 1.9900$), when *reheated* at about 200 K above the precipitation temperature, contained no visible extended defects. Thus images very similar to Fig. 1a were observed. It should be noted that neither the original quenched nor reheated specimens showed any diffuse scattering or other diffraction evidence for short-range ordering of small defects.

Table I indicates the range of D_{SP} and values obtained for each stoichiometry. In

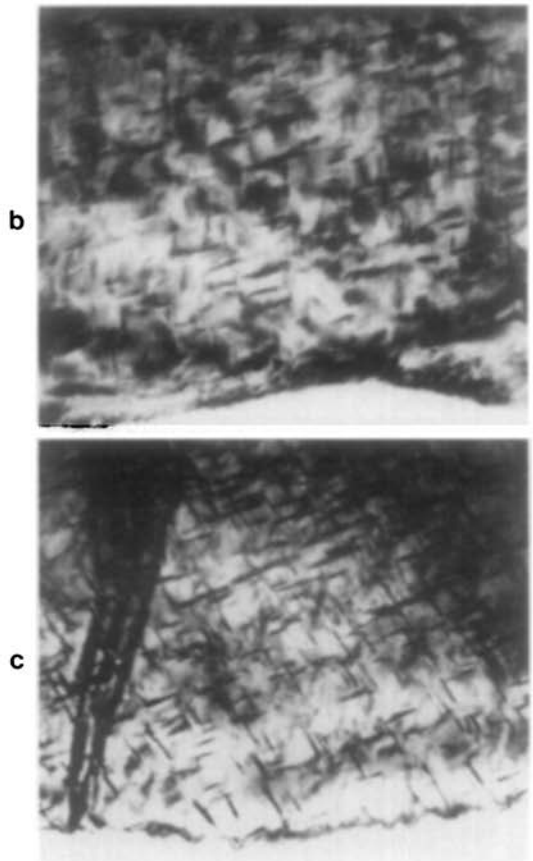

FIG. 1. Sequence showing time-evolution of precipitation phenomena in $(Ti,Cr)O_{1.98}$ after initial preparation at 1773 K (a); followed by annealing at 873 K 15 min (b); and 22 hr (c). (a) Shows *no* extended defects, (b) and (c) show intersecting {253} CSP. (c) shows, in addition, some extended fringe contrasts.

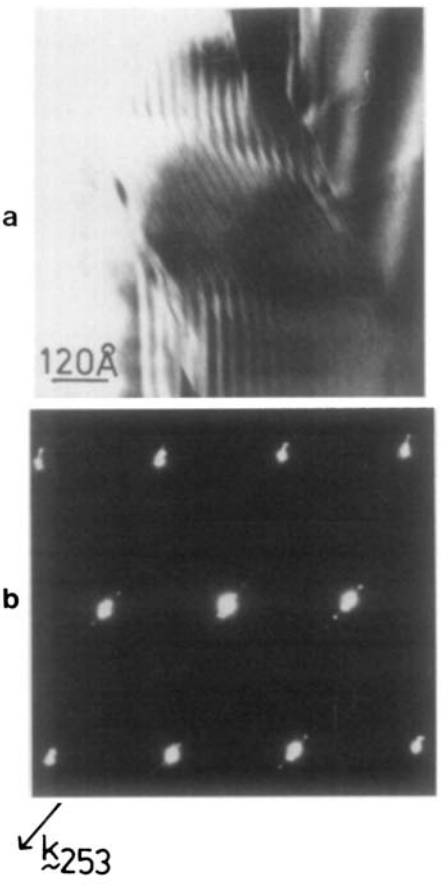

FIG. 2. (a) [111] Zone axis image showing {253} CSP lamellae in $(Ti,Cr)O_{1.98}$ after annealing just below the solubility limit (1073 K) for 24 hr. (b) Corresponding diffraction pattern showing rows of superlattice spots along $\mathbf{k}_{253}$, with CSP spacing $D_{CS} = 55$ Å, corresponding to stoichiometry $(Ti,Cr)O_{1.977}$.

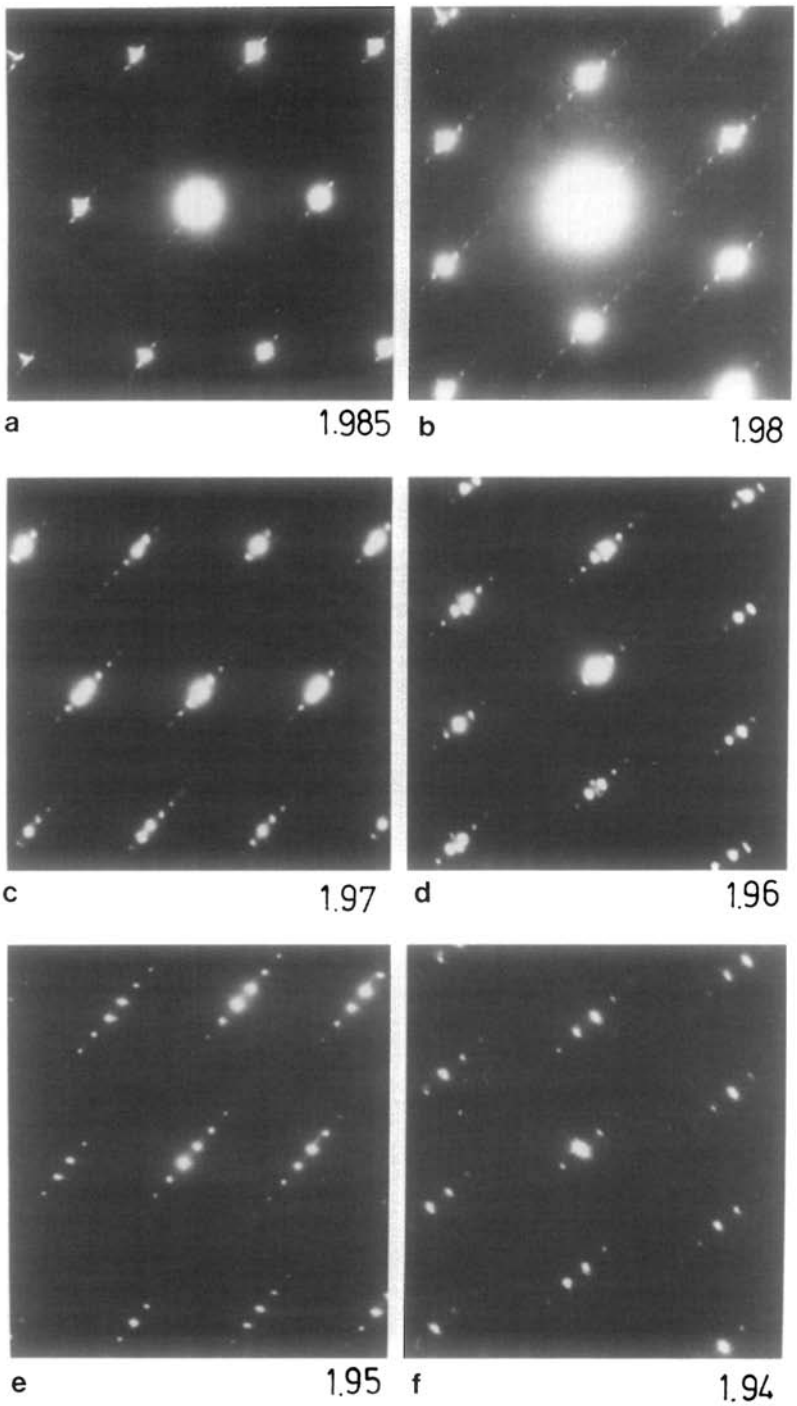

FIG. 3. (a–f) Series of [111] zone axis diffraction patterns obtained for different initial preparations (nominal stoichiometry indicated) after annealing at temperatures just outside the solid solubility limits. Note systematic change in superlattice spacings *without* change in orientation of CSP.

TABLE I

COMPARISON OF NOMINAL AND MEASURED STOICHIOMETRIES FOR DIFFERENT SPECIMEN PREPARATIONS

Nominal stoichiometry	Heat treatment (degree K)	Measured local stoichiometries	Mean measured stoichiometry
1.985	973	1.978	1.978
1.98	1173	1.977	1.977
1.97	1473	1.975	1.975
		1.975	
1.96	1573	1.970	1.970
1.93	1673	1.956	1.966
		1.966	
		1.965	
1.94	1773	1.960	1.9610
		1.9610	
		1.9620	
		1.9612	

Note. (1) Annealing times of 17–24 hr were used to produce reasonably well-ordered CSP spacings (cf. Fig. 3). (2) No CSP were observed for $y = 1.995$ or 1.990, even for temperatures of 470 K and times of up to 7 days. (3) Local stoichiometry is that measured from diffraction patterns of individual crystallites. (4) Mean stoichiometry is the average value obtained for a given heat-treated specimen.

most cases the results indicated reasonably homogeneous products. However, for most specimens there were significant differences between the prepared (nominal) bulk stoichiometries and those obtained after averaging a series of locally determined values. Shifts in stoichiometry may be expected due to (i) loss of chromia during the initial high-temperature reactions, e.g., at temperatures ≧ 1723°C (cf. Ref. (5)); (ii) local variations or inhomogeneities due to imperfect mixing or temperature gradients during initial reaction; and (iii) inaccuracies in weighings and/or loss of Cr_2O_3 powder during initial reaction, especially for stoichiometries very close to MX_2.

Table I represents the results of the analysis, and shows, for each annealing temperature, nominal and mean stoichiometries obtained by measuring D_{SP}. Figure 4 shows the results graphically. Specimens observed to contain *no* extended defects (open circles) and CSP lamellae (filled circles) are indicated.

IV. Discussion

(a) *Phase Limit for* $(Ti,Cr)O_{2-x}$

Uncertainties in D_{SP} of ~5% leads to errors of similar magnitude for x. The temperature measurement had precision of ca. ±20 K. However, the most significant source of uncertainty in determining the phase limit concerns the observed hysteresis of ≅200 K between precipitation and dissolution temperatures for a specimen of $(Ti,Cr)O_{1.975}$ (6). Thus whereas CSP precipitated on annealing at 1270 K or lower, these same CSP only dissolved completely after further annealing at 1470 K. Thus there is an uncertainty in the phase limit of ca. ±100 K. It was therefore not considered worthwhile to carry out further annealing

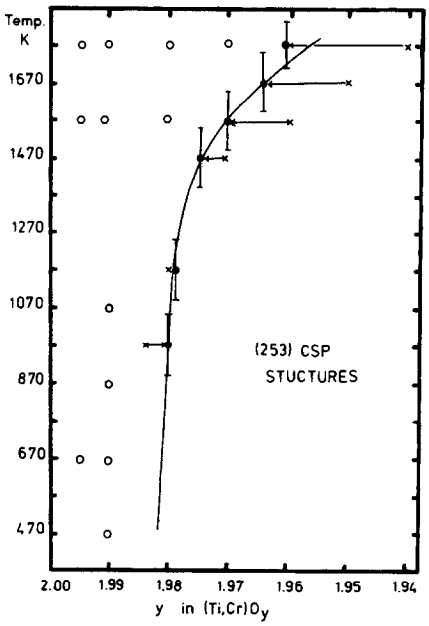

FIG. 4. Plot of observed local mean stoichiometrics (filled circles), and nominal initial stoichiometries (crosses) for samples observed to contain CSP lamellae after annealing at the temperatures indicated. Open circles represent samples which contained *no* visible extended defects. Solid line indicates the phase limit of $(Ti,Cr)O_{2-x}$. The error bars indicate uncertainty in the solid solubility limit due to hysteresis between CSP precipitation and dissolution temperatures.

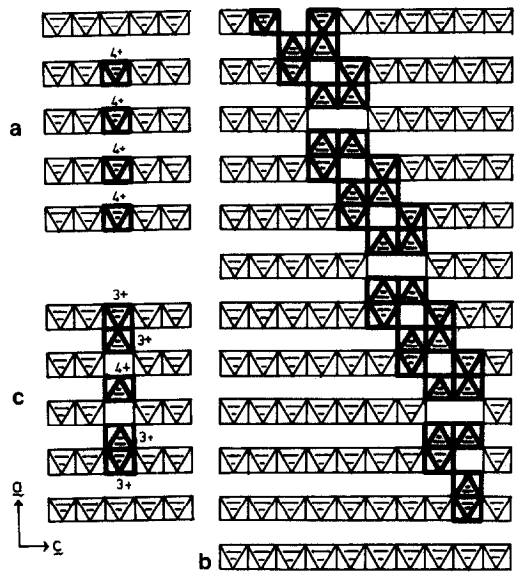

FIG. 5. (a). [010]-Bounded projection of rutile ($-\frac{1}{4} \leqq y \leqq \frac{1}{4}$) containing no defect; (b) corresponding projection of a (253) [011] CSP-pair in rutile, note face-sharing [MO_6]-octahedral sites (heavily lined); (c) linear cationic interstitial defect model derived from (b), note replacement of *three* Ti^{4+} sites (heavily lined in (a)) by *four* Cr^{3+} ions, forming two pairs of face-shared octahedra, linked by a displaced [TiO_6] octahedron.

runs designed to allow precipitation temperatures to be determined to higher accuracy. Thus, having obtained lamellae of CSP, upon annealing at temperature intervals of 100 K, it was assumed that the phase limit is given reasonably accurately by adding 100 K to the observed CSP onset temperature (Fig. 4). The error bars in Fig. 4 indicate the probable hysteresis region between precipitation and dissolution of CSP. Underlying reasons for hysteresis are discussed in Ref. (*6*), and involve the asymmetry in nucleation energy for precipitation of *pairs* of CSP compared with nucleation of a partial dislocation loop required for dissolution of *single* CSP. The observed differences between nominal and mean local stoichiometries also make it more difficult to achieve more accurate measurements of either precipitation or dissolution temperatures. For $(Ti,Cr)O_{2-x}$ ($x \leqq 0.015$) the gradient of the phase boundary is extremely steep (Fig. 4). Thus it was not easy to obtain further points in this region, given the observed shifts between nominal and local mean stoichiometries.

It is important to note that we were unable to obtain precipitation of extended defects in $(Ti,Cr)O_{1.990}$ and $(Ti,Cr)O_{1.995}$ preparations, even after annealing at temperatures in the range 520–900 K for periods of up to 7 days. Thus specimens having $x \leqq 0.010$ apparently lie within the nonstoichiometric phase $(Ti,Cr)O_{2-x}$, regardless of thermal history. Thus optical, "maser" and some other physical properties of this phase should be explicable in terms of small defects in this composition range.

A word of caution should be mentioned, however, that it is possible that low mobility of small defects in $(Ti,Cr)O_{2-x}$ ($x \leqq 0.01$) at temperatures $\leqq$ 620 K may underlie the observations in this region and hence relatively very long annealing may lead to precipitation of CSP.

(*b*) *Theoretical Model for the Nonstoichiometric Phase* $(Ti,Cr)O_{2-x}$

(*i*) *Small defect models.* Figure 5a depicts the [010]-bounded projection of rutile ($-\frac{1}{4} \leqq y \leqq \frac{1}{4}$), using an octahedral representation. High-resolution electron microscope (HREM) observations show that CSP precipitate predominantly as *pairs* in $(Ti,Cr)O_{2-x}$ ($x = 0.02$) (*9*), having *zero* net displacement vector. The corresponding representation for a pair of (253) CSP is given as Fig. 5b. Note that cations in face-shared octahedra have (formally, at least) charge +3, to account for the stoichiometry Ti_nO_{2n-2} of known members of the (253) family of structures (*4, 8*). The lack of ionic conductivity, due to charge-compensating lattice defects in chromia-doped rutile, prevented any definitive conclusion being made about the valence state of Cr ions

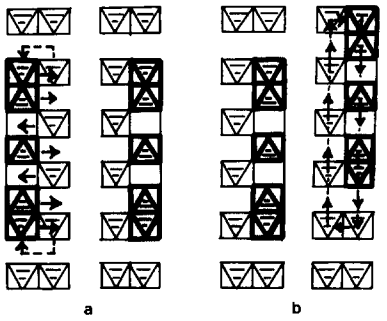

FIG. 6. Arrows indicate diffusion mechanisms required for movement of linear defects parallel to (a) [001] and (b) [010]. Note concerted atom shifts required for cooperative bulk diffusion of Cr^{3+} ions.

(*10*). Electrostatic valence arguments favor the location of Cr^{3+} ions in the face-shared octahedral sites indicated in Fig. 5b. Following arguments described earlier (*11*) we therefore take as our model for the small defects, presumably existing within the nonstoichiometric phase $(Ti,Cr)O_{2-x}$, the structural unit shown in Fig. 5c. This linear cationic interstitial defect consists of *two* pairs of face-shared octahedra, joined along [100] by a short segment containing one octahedron which is displaced from its normal site. Note that *three* of the original Ti^{4+} cations (indicated by thicker lines in Fig. 5a) have been replaced by *four* Cr^{3+} cations, giving zero net change in positive charge in the lattice. It is assumed that, upon doping, these small linear defects diffuse into the crystal to produce a homogeneous distribution of Cr^{3+}–Cr^{3+} pairs. Figures 6a and b indicate cooperative atom shifts which allow linear defect mobility along [001] and [100]. These jumps can always occur so that triple-face sharing of octahedra is avoided. Essentially only Frenkel-like defects are involved. (It was reported (*2*) that the ratio of diffusion coefficients for Cr^{3+} diffusion along [001] and [010] varies from ca. 4.0 at 1260 K to 1.75 at 1790 K.) Of course, if the activation energy for the reaction $Ti^{4+} + Cr^{3+} = Ti^{3+} + Cr^{4+}$ is not too great then the electrons originally (formally) attached to Cr^{3+} in face-shared octahedral sites may quickly become delocalized, especially at the formation temperatures (1773 K) used for chromia-doping rutile. Studies relating to the degree of delocalization, and possible ordering of Cr^{3+} into CSP, as a function of temperature, do not exist.

(*ii*) *Structure of the nonstoichiometric phase.* The occurrence of zero displacement (253) CSP-pairs as the predominant precipitation mechanism, on cooling of specimens across the phase boundary, and annealing, strongly suggests that the small defects existing within $(Ti,Cr)O_{2-x}$ are (predominantly) the linear defects drawn in Fig. 5c. These have length ~14 Å. The observation of disorder within CSP-pairs (*9*) is readily explained in terms of misalignments of linear defects with respect to ⟨111⟩ zone axes of the {253} CSP (*11*). The linear defects (Fig. 5c) may readily elongate along ⟨100⟩ by diffusive hops parallel to ⟨100⟩ (see Fig. 1 of Ref. (*11*)). Hence it is considered likely that a statistical distribution of linear defects, some shorter, but mostly longer than Fig. 5c, is likely to occur, with the details of the distribution being both temperature and stoichiometry dependent. It should also be realized that both [100] and [010] linear defects are involved, since these are symmetrically equivalent, giving rise to additional possibilities for internal disorder and the production of pinning defects, involving intersections of [100] and [010] defects. A dynamic equilibrium is readily visualized, whereby mobile small defects are continuously changing length and orientation at high temperature (Figs. 9a,b of Ref. (*6*) depicts atomic mechanisms for interconversion of [010] and [100] defects).

(*c*) *Aggregation Mechanisms Involving Small Defects*

As shown above (see Fig. 5b), a pair of (253) CSP may readily form in the bulk of a

homogeneously doped crystal. Since there is zero lattice displacement across such a CSP-pair, nucleation is relatively easy compared with an interstitial dislocation loop mechanism. It should be appreciated that, once formed, CSP-pairs tend to split or separate (atomic mechanisms are described in Ref. (*12*)) forming eventually an ordered Ti_nO_{2n-p} (n,p integers (*4, 8*)) CSP structure. (CSP dissolution mechanisms and an explanation for the observed temperature hysteresis for precipitation/dissolution are discussed in Ref. (*6*).)

Precipitation of CSP by oxygen vacancy defects is also readily imagined (*13*), involving the collapse of a vacancy disk with partial dislocation having Burger's vector $\mathbf{b} = \langle 0\ -\frac{1}{2}\ \frac{1}{2}\rangle$. Alternatively, precipitation of a CSP-pair by a vacancy mechanism would involve Burger's vector $\mathbf{b} = \langle 011\rangle$, and a very much greater nucleation energy. The HREM evidence (*9*) that CSP-pair precipitation predominates, with *zero* net displacement vector, effectively rules out the possibility of a vacancy defect mechanism.

V. Conclusion

The present observations, with supporting evidence from *in situ* (*6*) and HREM observations (*9*), and their interpretation in terms of small defect models, lead to the following conclusions:

(i) It is established that the phase (Ti, Cr)O_{2-x} is *genuinely* nonstoichiometric—in the sense that the stoichiometry range is due to small defects, which are coherent with the rutile lattice and highly mobile within it, and effectively homogeneous and random in their distribution;

(ii) The stoichiometry dependence of CSP-precipitation temperature, based upon electron microscopic observations, has allowed the phase limits to be effectively determined as a function of temperature (Fig. 4).

Acknowledgments

This work was supported by the Australian Research Grants Committee and the University of Melbourne. The authors are grateful for the valuable collaborations of Dr. M. G. Blanchin (Lyon) and Dr. D. J. Smith (HREM Laboratory, Cambridge).

References

1. O. W. Flörke and Chihming Wang Lee, *J. Solid State Chem.* **1,** 445–453 (1970).
2. M. O'Keeffe and T. J. Ribble, *J. Solid State Chem.* **4,** 351–356 (1971).
3. R. M. Gibb and J. S. Anderson, *J. Solid State Chem.* **4,** 379–390 (1972).
4. D. K. Philp and L. A. Bursill, *J. Solid State Chem.* **10,** 357–370 (1974).
5. S. Somiya, S. Hirano, and S. Kamiya, *J. Solid State Chem.* **25,** 273–284 (1978).
6. L. A. Bursill and M. G. Blanchin, submitted for publication.
7. M. G. Blanchin, L. A. Bursill, J. L. Hutchison, and P. L. Gai, *J. Physique, Colloq.* C3, **42,** C3/95–112 (1981).
8. D. K. Philp and L. A. Bursill, *Acta Crystallogr. A* **30,** 265–272 (1974).
9. L. A. Bursill, D. J. Smith, and M. G. Blanchin, in preparation.
10. E. Tani and J. F. Baumard, *J. Solid State Chem.* **32,** 105–113 (1980).
11. L. A. Bursill and M. G. Blanchin, *J. Phys. (Lettres)* **44,** L165–170 (1983).
12. M. G. Blanchin, L. A. Bursill, and D. J. Smith, *Proc. Roy. Soc. (London)*, in press.
13. L. A. Bursill, *Prog. Solid State Chem.* **7,** 177–253 (1972).